

Challenge for describing the cluster states starting with realistic interaction

Naoyuki Itagaki,¹ Tokuro Fukui,¹ and Akihiro Tohsaki²

¹*Yukawa Institute for Theoretical Physics, Kyoto University,
Kitashirakawa Oiwake-Cho, Kyoto 606-8502, Japan*

²*Research Center for Nuclear Physics (RCNP), Osaka University,
10-1 Mihogaoka, Ibaraki, Osaka 567-0047, Japan*

(Dated: March 20, 2020)

We aim to describe the cluster states of nuclear systems starting with a realistic interaction, which is a challenge of the modern nuclear theories. Here, the short-range correlation of realistic interaction is treated by employing the damping factor, and the resultant interaction can be applied to the cluster structure of light nuclei. We start with a realistic interaction (G3RS) and transform it in this way, and the α - α energy curve is compared with the results of phenomenological interactions. The attractive effect between two α 's is found to be not enough even with a damping factor for the short-range repulsion, and the necessity of a finite-range three-body term is discussed. With this three-body term, the resonance energy of the ground state and the scattering phase shift of two α 's can be reproduced. Also, the binding energy of ^{16}O from the four α threshold is reasonably reproduced. The linear-chain structure of three and four α clusters in ^{12}C and ^{16}O are calculated with this interaction and compared with the results of the conventional approaches including the density functional theories.

I. INTRODUCTION

Describing the cluster states starting with the realistic interactions is a challenge of the modern nuclear theories. The ^4He nucleus is a strongly bound many-nucleon system in the light mass region, thus the α clusters can be basic building blocks of the nuclear structure. The α cluster models [1, 2] have been developed and applied in numerous works for the description of cluster structures such as 3α clustering in the so-called Hoyle state of ^{12}C [3–5]. In most of the conventional cluster models, each α cluster is assumed as a simple $(0s)^4$ configuration. However, in the real systems, nucleons are correlated owing to the repulsive core in the short-range part of the central interaction, and this effect is not explicitly treated in the conventional cluster models. These days, such NN correlation is widely discussed based on modern *ab initio* theories not only in very light nuclei but also in medium-heavy nuclei [6]. Most of the *ab initio* theories have been developed based on the shell-model point of view, and describing cluster states is a challenge of the modern *ab initio* ones [7–9], since a quite large model space is required.

Concerning the description of the cluster states starting with realistic interactions, one of the ways is to utilize Fermionic molecular dynamics (FMD) combined with the unitary correlation operator method (UCOM) [10, 11]. In UCOM, the effects of the short-range correlation are included with the unitary transformation of the Hamiltonian, which in principle induces many-body operators up to the A -body level, with the mass number A since we need to expand this unitary operator for the calculation of the expectation values of the norm and the Hamiltonian. We aim to treat the short-range correlation caused by the repulsive core of the central interaction in a simple way without performing the unitary transformation and expanding the exponents.

The assumption of the $(0s)^4$ configuration for the α clusters in the conventional α cluster models also prevents us to include the contribution of the non-central interaction. We have previously introduced antisymmetrized quasi cluster model (AQCM) [12–19] and tensor version of AQCM (AQCM-T) [20–23] to include the contribution of the non-central interactions in the α -cluster model by breaking the $(0s)^4$ configuration properly. It has been discussed that the tensor suppression effect at small α - α distances works repulsively and plays an important role in the appearance of the α cluster structures [20, 21, 23]. In this paper, however, we do not touch into the non-central interactions, since we are interested only in the short-range correlation originating from the central interaction. Therefore, here the model space is the conventional Brink model with the $(0s)^4$ configuration for each α cluster. In return, we start with a realistic interaction, G3RS (Gaussian three-range soft-core potential) [24] for the central part.

Until now, in conventional cluster model studies, phenomenological interactions, such as Volkov interaction [25], have been widely used, which allows us to reproduce the α - α scattering phase shift by properly choosing the Majorana exchange parameter. However, the realistic and phenomenological interactions are quite different. First of all, the realistic interactions have short-range cores, which makes the application to many-body systems extremely difficult. Also, they have quite different interaction ranges. Most of the realistic interactions have the energy minimum point around $r \sim 1$ fm, where r is the relative distance between the nucleons. In contrast, the ranges of the conventional interactions for the cluster studies are much larger; for instance, the attractive term of the Volkov No.2 interaction has the range of 1.80 fm, which creates the energy minimum point around $r \sim 1.3$ fm for the even-parity state. Therefore, the attractive effect has much longer ranges in the phenomeno-

logical interactions. It is quite interesting to investigate how the cluster structures appear with realistic interactions, which have completely different ranges.

In this paper, we discuss the cluster states of light nuclei starting with the realistic interaction. The short-range correlation of the realistic interaction is treated by employing the damping factor. Using an interaction transformed in this way, the α - α energy curve and the scattering phase shift are calculated, which are compared with the results of phenomenological interactions. It is quite well known that the phenomenological interaction should have proper density dependence in order to satisfy the saturation property of nuclear systems. The Tohsaki interaction, which has finite-range three-body terms [15, 26, 27], satisfies the saturation properties. We employ this interaction as a phenomenological one, which gives a reasonable size and binding energy of the α cluster in addition to the α - α scattering phase shift.

Then the interactions introduced here are applied to the linear-chain states of α clusters. There has been a long history of both theoretical and experimental studies for the possibility of α chain states [28]. Once the second 0^+ state of ^{12}C just above the three- α threshold energy has been assigned as a candidate, but now the state is regarded as an α gas state [4, 29]. In return, not exactly linear but bent chain was suggested around $E_x \sim 10$ MeV region corresponding to 3 MeV above the three α threshold [10, 30, 31]. Furthermore, the possibility of four- α and six- α chain state was suggested [32, 33]. It has been theoretically discussed that the main decay path of the linear-chain states passes through the bending motion, and adding valence neutrons and/or giving angular momentum to the system work to prevent this motion [34–49]. Not only cluster models, but recently various mean-field approaches are also successfully applied to discuss the stability of the linear-chain configurations.

This paper is organized as follows; in Sec. II, the framework, especially for the model wave function and the Hamiltonian of the present model, is described. In Sec. III, we introduce the damping factor for the short-range part of the central interaction, and the α - α energy curve and scattering phase shift are calculated and compared with the results of a phenomenological interaction with finite-range three-body terms (**A.**). Also the linear-chain structure of three and four α clusters in ^{12}C and ^{16}O are calculated and compared with the results of the conventional approaches (**B.**). The summary is presented in Sec. IV.

II. METHOD

A. wave function (Brink model)

Here we employ the conventional Brink model [1] for the α cluster states. In the Brink model, each single-

particle wave function is described by a Gaussian,

$$\phi_{ij} = \left(\frac{2\nu}{\pi}\right)^{\frac{3}{4}} \exp\left[-\nu(\mathbf{r} - \mathbf{R}_i)^2\right] \chi_j, \quad (1)$$

where the Gaussian center parameter \mathbf{R}_i shows the expectation value of the position of the particle, and χ_j is the spin-isospin wave function. The size parameter ν is chosen to be 0.25 fm^{-2} , which reproduces the observed radius of ^4He . Here, four single particle wave functions with different spin and isospin sharing a common Gaussian center parameter \mathbf{R}_i correspond to an α cluster. The Slater determinant of the Brink model is constructed from these single particle wave functions by antisymmetrizing them,

$$\Phi_{SD}(\mathbf{R}_1, \mathbf{R}_2, \dots, \mathbf{R}_N) = \mathcal{A}\{(\phi_{11}\phi_{12}\phi_{13}\phi_{14})(\phi_{21}\phi_{22}\phi_{23}\phi_{24}) \dots (\phi_{N1}\phi_{N2}\phi_{N3}\phi_{N4})\}. \quad (2)$$

This is the case that we have N α clusters and the mass number A is given by $A = 4N$. This assumption of common Gaussian center parameter for four nucleons removes the contribution of the non-central interactions, spin-orbit and tensor components, after the antisymmetrization.

For ^8Be we introduce two α clusters, and two Gaussian center parameters are introduced as $\mathbf{R}_1 = d\mathbf{e}_z/2$ and $\mathbf{R}_2 = -d\mathbf{e}_z/2$ with the relative distance of d , where \mathbf{e}_z is the unit vector for the z direction. For the ground state of ^{16}O , the Gaussian center parameters are introduced to have a tetrahedron shape with a fixed relative distance d . In both cases, the Slater determinants with different d values are superposed based on the generator coordinate method (GCM) [1].

Also, the linear chain configurations of three and four α clusters in ^{12}C and ^{16}O can be calculated by assuming one-dimensional configurations for the $\{\mathbf{R}_i\}$ values. The distances between the α clusters are randomly generated, and these Slater determinants are superposed based on the GCM.

The Slater determinants are projected to the eigen states of the angular momenta by numerical integration,

$$\Phi_{MK}^J = \frac{2J+1}{8\pi^2} \int d\Omega D_{MK}^J{}^* R(\Omega) \Phi_{SD}, \quad (3)$$

where D_{MK}^J is Wigner D-function and $R(\Omega)$ is the rotation operator for the spatial and spin parts of the wave function. This integration over the Euler angle Ω is numerically performed.

B. Hamiltonian

The Hamiltonian used in the present calculation is

$$\hat{H} = \sum_i^A \hat{T}_i - \hat{T}_G + \sum_{i<j}^A \left[\hat{V}_c(i,j) + \hat{V}_{\text{Coulomb}}(i,j) \right], \quad (4)$$

where \hat{T}_i is the kinetic energy operator of i th nucleon, and the total kinetic energy operator for the cm motion (\hat{T}_G) is subtracted. The two-body interaction consists of only the central interaction (\hat{V}_c) and Coulomb interaction (\hat{V}_{Coulomb}), since the effect of the non-central interactions disappear in the α cluster model. This above Hamiltonian is relevant for the G3RS interaction, which is a realistic interaction. However, to reduce the height of the short-range core part. For the region of $r \leq r_0$, the factor $F(r)$ is multiplied to the central part of the G3RS interaction. Also, we examine the effect of the finite-range three-body interaction.

We compare the results obtained with a phenomenological interaction, Tohsaki F1 interaction [15, 26, 27]. This interaction also contains finite-range three-body terms.

III. RESULTS

A. introduction of the damping factor

For the central interaction \hat{V}_c , we use the G3RS interaction [24], which is the realistic interaction designed to reproduce the scattering phase shift of the nucleon-nucleon scattering up to around 600 MeV. The central part of G3RS has three-range Gaussian form as

$$\begin{aligned} \hat{V}_c = & \hat{P}_{ij}(^3E) \sum_{n=1}^3 V_{c,n}^3 E \exp\left(-\frac{r_{ij}^2}{\eta_{c,n}^2}\right) \\ & + \hat{P}_{ij}(^1E) \sum_{n=1}^3 V_{c,n}^1 E \exp\left(-\frac{r_{ij}^2}{\eta_{c,n}^2}\right) \\ & + \hat{P}_{ij}(^3O) \sum_{n=1}^3 V_{c,n}^3 O \exp\left(-\frac{r_{ij}^2}{\eta_{c,n}^2}\right) \\ & + \hat{P}_{ij}(^1O) \sum_{n=1}^3 V_{c,n}^1 O \exp\left(-\frac{r_{ij}^2}{\eta_{c,n}^2}\right), \end{aligned} \quad (5)$$

where $\hat{P}_{ij}(^1,^3E)$ and $\hat{P}_{ij}(^1,^3O)$ are the projection operators to the $^1,^3E$ (singlet-even, triplet-even) and $^1,^3O$ (singlet-even, triplet-odd) states, respectively. The parameter set of “case 1” in Ref. [24] is listed in Table I.

The spatial part of the G3RS interaction as functions of the nucleon-nucleon distance r is shown in Fig. 1. Here,

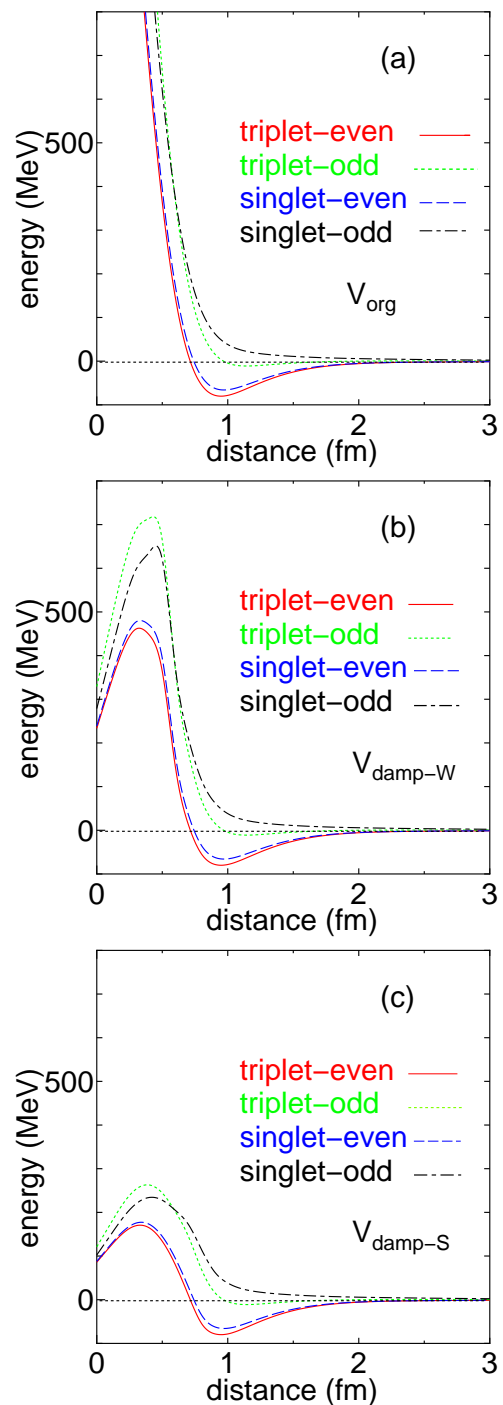


FIG. 1. The spatial part of the G3RS interaction as functions of the nucleon-nucleon distance r (“case 1” in Ref. [24]). (a): V_{org} , the original form, (b): V_{damp-W} , with weaker damping factor, $r_0 = 0.5$ fm and $m = 2$ in Eq. (6), and (c): V_{damp-S} , with stronger damping factor, $r_0 = 0.75$ fm and $m = 3$ in Eq. (6).

TABLE I. The parameter sets for the central part of the G3RS interaction. The parameter set “case 1” in Ref. [24] is adopted.

n	1	2	3
$\eta_{c,n}$ (fm)	2.5	0.942	0.447
$V_{c,n}^{3E}$ (MeV)	-5	-210	2000
$V_{c,n}^{1E}$ (MeV)	-5	-270	2000
$V_{c,n}^{3O}$ (MeV)	1.6667	-50	2500
$V_{c,n}^{1O}$ (MeV)	10	50	2000

Fig. 1 (a) is the original form of the G3RS interaction, which is called V_{org} . This is the realistic interaction and has a short-range core part. For the use of the calculation of the many-body system, here we introduce a damping factor to reduce the height of the short-range core part (around 2500 MeV). This is equivalent to the regularization in the momentum space to suppress the high-momentum contribution (see, for instance Ref. [50] for the regularization in the chiral effective field theory). For the region of $r \leq r_0$, the factor $F(r)$ is multiplied to the central part of the G3RS interaction;

$$F(r) = 1/(\exp[1 - r/r_0])^m. \quad (6)$$

This damping factor is unity in the region of $r \geq r_0$ but start changing at $r = r_0$ and converges to e^{-m} at $r = 0$. In this article, we compare two parameter sets; weaker damping factor and stronger one. For the weaker damping factor, the values of $r_0 = 0.5$ fm and $m = 2$ are adopted. The resultant G3RS interaction is called V_{damp-W} and the form is shown in Fig 1 (b). This is the G3RS interaction after multiplying the damping factor in the region of $r \leq 0.5$ fm, and the short-range core is reduced. We also introduce stronger damping factor, which has the parameters of $r_0 = 0.75$ fm and $m = 3$ and is called V_{damp-S} . Figure 1 (c) shows the shape after multiplying the damping factor. As we can see, when two nucleons get closer, the damping starts already at $r = 0.75$ fm and the inner part is drastically reduced.

Using these interactions, the 0^+ energy curves of two α clusters (^8Be) are calculated and shown in Fig. 2. At first, we show the energy curves of the phenomenological interactions, which are known to well reproduce the α - α scattering phase shift. The dotted line and dashed line in Fig. 2 (a) are results of the Volkov No.2 interaction [25] with the Majorana exchange parameter of $M = 0.6$ and Tohsaki F1 interaction [26], respectively. The horizontal axis shows the distance between the two α clusters, and the energy is measured from the two α threshold. These two lines are very similar, and both of them have the energy minimum points around the α - α distance of 4 fm. This is coming from the long-range nature of these phenomenological interactions. The energy does not become zero even at the large relative distances owing to the zero-point kinetic energy ($\hbar\omega/4 \sim 5$ MeV), which is the kinetic energy for fixing the relative distance.

Next, the energy curves of α - α calculated with the G3RS interaction are shown in Fig. 2 (b). The energy of each α cluster indeed depends on the interactions, but again here the energy is measured from the two- α threshold. The dotted line is the result of the original G3RS interaction, V_{org} (Fig. 1 (a)). Due to the repulsive effect at short relative distances, the energy minimum point around the relative distance of 4 fm found in Fig. 2 (a) does not appear. This energy minimum point cannot be obtained even if we reduce the short-range repulsion by introducing the damping factor for the nucleon-nucleon interaction, as in the dashed line, where V_{damp-W} is adopted; the energy around the α - α distance of 4 fm is constant around 6 MeV. Rather surprisingly, this situation does not change even if we adopted a much stronger damping factor. The dash-dotted line shows the result of V_{damp-S} , and even if the repulsive effect is reduced at short α - α distances, the energy around 4 fm is still constant around 6 MeV. Experimentally, the ground 0^+ state of ^8Be is located at 0.09184 MeV, and the α - α energy within the region inside the Coulomb barrier is essential for the reproduction of this value. If we superpose Slater determinants with different α - α distances (1, 2, 3, ..., 10 fm) based on the GCM, the obtained energy of the ground 0^+ state does decrease by a few MeV. Nevertheless, it is still above the α - α threshold by 1-2 MeV in the cases of V_{org} , V_{damp-W} , and even V_{damp-S} . Without the reproduction of this ground state energy, we cannot discuss the scattering phase shift, which is quite sensitive to the energy of the resonance state from the threshold. Therefore, we need an additional effect other than reducing the short-range repulsion by introducing the damping factor, which contributes to the lowering the energy around the α - α distance of 4 fm.

One may consider that the missing of the tensor interaction due to the assumption of $(0s)^4$ configuration for each α cluster is the origin of the shortage of attractive effect. However, as we discussed based on the AQQM-T [20, 21], the attractive effect of the tensor interaction is very strong inside each ^4He rather than between the two ^4He nuclei, when two ^4He nuclei are far with each other. This tensor effect is blocked when two ^4He approach, which works repulsively. One of the other mechanisms, which contributes to the lowering of the energy around the α - α distance of 4 fm, is three-body nuclear interaction. Here we adopt a finite-range three-body interaction V_{f3b} ,

$$V_{f3b} = \frac{1}{6} \sum_{i \neq j, j \neq k, i \neq k} V_{ijk}^{(3)}, \quad (7)$$

where,

$$V_{ijk}^{(3)} = V^{(3)} \exp[-\mu(\vec{r}_i - \vec{r}_j)^2 - \mu(\vec{r}_i - \vec{r}_k)^2] \times (W + MP_{ij}^r)(W + MP_{ik}^r). \quad (8)$$

The parameters involved in Eq. (8) are fixed phenomenologically in order to account for the 2- α system, as well as the properties of ^{16}O . The strength $V^{(3)}$ and the range

μ are set to -9 MeV and 0.1 fm^{-2} , respectively. The strength is small, but it has a very long range. The Majorana exchange parameter M is set to 0.645 and $W = 1 - M$. The operator P_{ij}^r exchanges the spatial part of the wave functions of the interacting i -th and j -th nucleons. The introduction of this Majorana term is needed for the reproduction of the binding energy of ^{16}O from the four- α threshold, which will be discussed shortly. With this phenomenological three-body nucleon-nucleon interaction, we do not need to drastically reduce the short-range repulsion of the two-body interaction, thus we adopt weaker damping factor, $V_{\text{damp}-W}$ (extremely strong damping factor gives poor reproduction of the α - α scattering phase shift). The α - α energy curve calculated with $V_{\text{damp}-W} + V_{f3b}$ is shown as the solid line in Fig. 2 (b). The energy minimum point appears around the α - α distance of 4 fm, and the shape is very similar, apart from the short-distance region, to the results of the phenomenological interactions shown in Fig. 2 (a), which reproduce the α - α scattering phase shift.

The α - α scattering phase shift (^8Be) is calculated and shown in Fig. 3 ((a): 0^+ , (b): 2^+ , and (c): 4^+) as a function of the center of mass energy of two α 's. This is calculated using the Kohn-Hulthén variational principle combined with the GCM [51, 52]. The solid lines show the results of $V_{\text{damp}-W} + V_{f3b}$, and the dashed lines are obtained with the Tohsaki F1 interaction, which is designed to reproduce the α - α scattering phase shift. The experimental data (open circles) are taken from Ref. [53], where the measured data were compiled from the original works [54–60]. The reproduction of the data is not perfect and the repulsive effect is a bit stronger in the cases of $V_{\text{damp}-W} + V_{f3b}$, but the basic trend of the scattering phase shift can be satisfied.

Figure 4 shows the 0^+ energy of ^{16}O . Here tetrahedron configuration of four α clusters is assumed, and the horizontal axis shows the distance between the two α clusters. The dotted, dashed, and dot-dashed lines are respectively associated with V_{org} , $V_{\text{damp}-W}$, and $V_{\text{damp}-S}$. The solid line is the result by $V_{\text{damp}-W}$ with finite-range three-body interaction ($V_{\text{damp}-W} + V_{f3b}$), and the energy minimum point appears at the α - α distance of 2.5-3.0 fm. Experimentally, the ground state of ^{16}O is lower than the four- α threshold energy by 14.4 MeV, and the solid line is close to this value. We superpose the Slater determinants with different α - α distances based on the GCM, and the ground 0^+ state is obtained at -16.2 MeV. The matter radius is obtained as 2.52 fm corresponding to the charge radius of 2.65 fm (experimentally 2.69 fm).

B. linear-chain states

The interaction introduced in the last subsection can be applied to the linear-chain configurations of three and four α clusters in ^{12}C and ^{16}O . The rotational band structure of the linear-chain structure of the three α clusters (^{12}C) is shown in Fig. 5. The Slater determi-

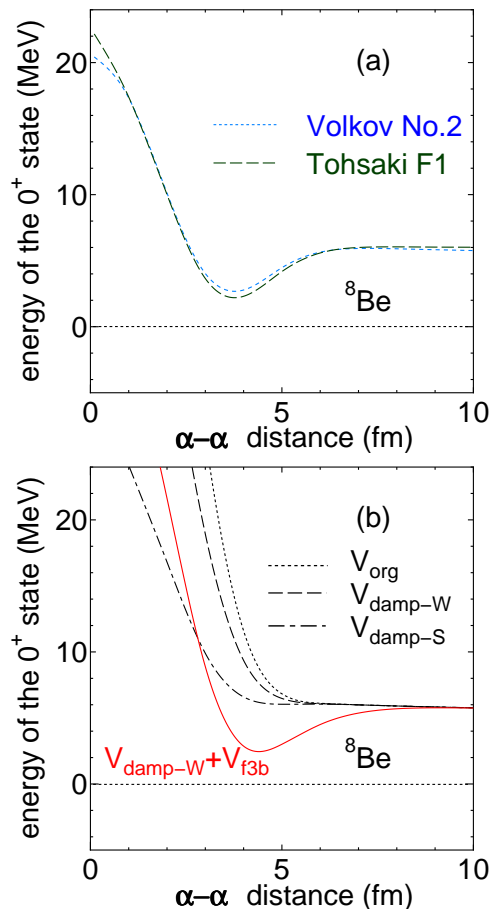


FIG. 2. The 0^+ energy curves of two α clusters (^8Be). The energy is measured from the two α threshold. The horizontal axis shows the distance between the two α clusters. (a): the dotted and dashed lines are obtained with the Majorana exchange parameter of $M = 0.60$ and Tohsaki F1 interaction, respectively. (b): the dotted, dashed, and dot-dashed lines are results of V_{org} , $V_{\text{damp}-W}$, and $V_{\text{damp}-S}$, respectively. The solid line corresponds to the result by $V_{\text{damp}-W}$ with a finite-range three-body term ($V_{\text{damp}-W} + V_{f3b}$).

nants with different distances between α clusters within one-dimensional configurations are randomly generated and superposed based on the GCM. The energy is measured from the three α threshold. The horizontal axis is $J(J+1)$, where J is the angular momentum of the system. The solid circles show the result of $V_{\text{damp}-W} + V_{f3b}$ and open circles correspond to that of Tohsaki F1. The band head energy is 8.9 MeV for $V_{\text{damp}-W} + V_{f3b}$ (solid circle), and Tohsaki interaction gives 7.2 MeV (open circle). Experimentally the three- α threshold energy corresponds to $E_x = 7.4$ MeV, thus these band head energies correspond to $E_x = 16 - 17$ MeV from the ground state. The band head energy was estimated as $E_x = 16.6$ MeV (measured from the ground state) in the covariant density functional approach [45] and $E_x = 10.1$ MeV (measured from the three- α threshold) in a modern cluster

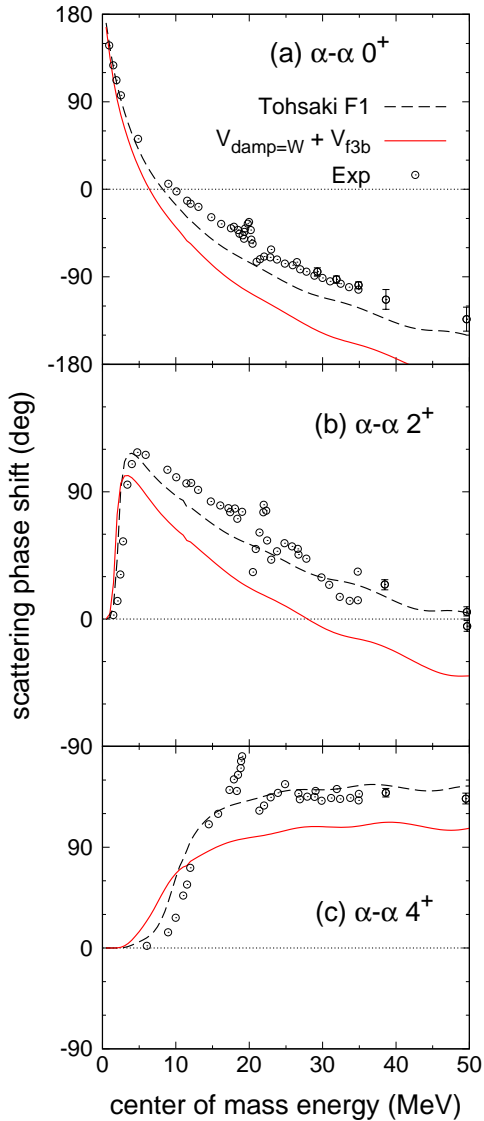


FIG. 3. The α - α scattering phase shifts as a function of the center of mass energy between two α 's, (a): 0^+ , (b): 2^+ , and (c): 4^+ . The solid lines show the results of $V_{damp-W} + V_{f3b}$, and the dashed lines are those of Tohsaki F1 interaction [26]. The experimental data (open circles) are taken from Ref. [53], where the measured data were compiled from the original works [54–60].

model [44]. Our results of both $V_{damp-W} + V_{f3b}$ and Tohsaki F1 almost agree with these. The slope of the rotational band ($\hbar^2/2I$, I the moment of inertia) is obtained as 102 keV and 119 keV for the solid and open circles, respectively, if we just average between the 0^+ and 8^+ energies. However in the high-spin states, where the centrifugal force is strong, the α - α distance gets larger, which creates a decrease of the slope. This is in ^{14}C and not ^{12}C , but the slope of $\hbar^2/2I \sim 120$ keV was reported in Ref. [61].

The rotational band structure of the linear-chain struc-

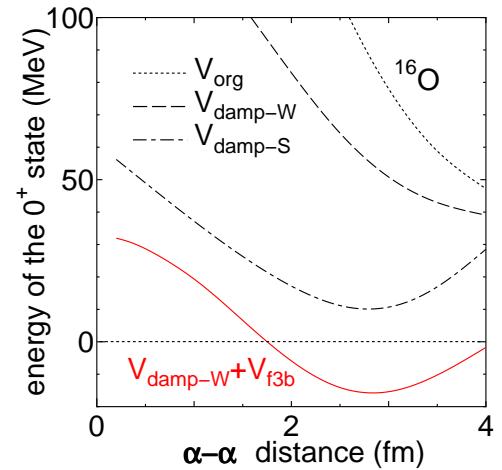


FIG. 4. The 0^+ energy curves of ^{16}O with the tetrahedron configuration of four α clusters as a functions of the relative α - α distance d . The energy is measured from the four α threshold. The lines are the same as in Fig. 2.

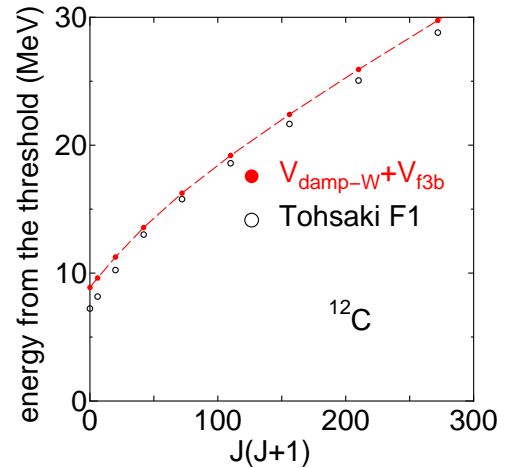


FIG. 5. The rotational band structure of the linear-chain structure of the three α clusters (^{12}C). The energy is measured from the three- α threshold. The horizontal axis is $J(J+1)$, where J is the angular momentum of the system. The solid circles show the result for $V_{damp-W} + V_{f3b}$. The open circles are the result obtained with a phenomenological interaction, Tohsaki F1 [26].

ture of the four α clusters (^{16}O) is shown in Fig. 6. Again the Slater determinants with different distances between α clusters are randomly generated and superposed based on the GCM, and the energy is measured from the four α threshold. The horizontal axis is $J(J+1)$, where J is the angular momentum of the system. The solid circles show the result of $V_{damp-W} + V_{f3b}$ and the open circles are associated with Tohsaki F1. The band head energy measured from the four- α threshold energies are 19.4 MeV and 16.7 MeV for the solid and open circles, respectively. If we measure the energy from the ground state, $V_{damp-W} + V_{f3b}$ (solid circle) give the band head energy

of 35.6 MeV. The slope of the rotational band again decreases in the high-spin states due to the large centrifugal force (an increase of the α - α distance). The solid circles give the value of the slope as 0.051 MeV between the 0^+ and 10^+ states (open circles give 0.063 MeV). These interactions give similar results.

These days, the linear-chain states of four α clusters are discussed also with various density functional theories [41, 42]. Among them, nonrelativistic Hartree-Fock approaches are adopted in Refs. [34, 36, 41], and the band head energy of ~ 40 MeV from the ground state, which agrees with the results of the present study, was reported [41]. The slope of $\hbar^2/2I = 0.06 - 0.08$ MeV was suggested there. A covariant framework predicted the band head energy of ~ 30 MeV and the slope of $\hbar^2/2I = 0.11$ MeV [42]. Similar values are obtained by the modern cluster model studies [44, 46].

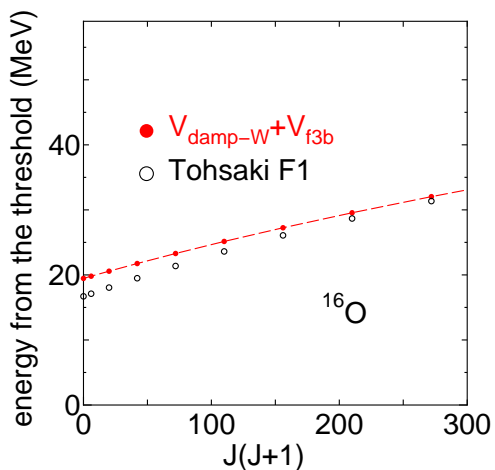


FIG. 6. The rotational band structure of the linear-chain structure of the four α clusters (^{16}O). The energy is measured from the four α threshold. The circles are the same as in Fig. 5.

IV. CONCLUSION

We investigated the cluster states of light nuclei starting with the realistic interaction, G3RS. The short-range correlation of the realistic interaction was treated by employing a damping factor. Using an interaction transformed in such a way, the α - α energy curve and the scattering phase shift were calculated. Although the original G3RS interaction shows too repulsive features, the scat-

tering phase shift is reasonably reproduced after introducing the damping factor. The inclusion of a finite-rang three-body interaction gives the energy minimum point of the α - α energy curve around the relative distance of 4 fm as in the case of the phenomenological interaction. This allows the reproduction of the ground-state energy, which is essential for describing the scattering phase shift, but this energy minimum point does not appear without the three-body effect even with a very strong damping factor for the short-range repulsion of the two-body interaction. With this three-body term, it is capable of reproducing the binding energy of four α clusters from the threshold in ^{16}O .

The rotational band structure of the linear-chain structure of the three α clusters (^{12}C) can be calculated, and the band head energy was obtained at 8.9 MeV from the three- α threshold energy in the case of G3RS interaction with the three-body interaction. This result well agrees with those by other conventional approaches. Similarly, the linear-chain structure of the four α clusters (^{16}O) can be calculated and the band head energy was calculated at ~ 36 MeV. These days, the linear-chain states of four α clusters are discussed also with various density functional theories, which predicted the band head energies of 30 \sim 40 MeV from the ground state, in agreement with the result of the present study. The slope of the rotational band structure of the G3RS interaction also almost agrees with the phenomenological cluster models and density functional theories.

As future works, using the interaction proposed here, light neutron-rich nuclei can be calculated. The strength of the three-body interaction should be carefully determined, and introducing Heisenberg and Bartlett exchange terms is the possible way to keep the consistency with the present results. Also, deriving an effective interaction consisting of the two- and three-body terms for the cluster model in a more microscopic way is quite an important task. We are working along this line based on the chiral effective field theory.

ACKNOWLEDGMENTS

We thank Professor M. Kamimura for the calculation of the scattering phase shift. The numerical calculation has been performed using the computer facility of Yukawa Institute for Theoretical Physics, Kyoto University and Research Center for Nuclear Physics, Osaka University.

-
- [1] D. M. Brink, Proc. Int. School Phys. “Enrico Fermi” **XXXVI**, 247 (1966).
 [2] Y. Fujiwara, H. Horiuchi, K. Ikeda, M. Kamimura, K. Katō, Y. Suzuki, and E. Uegaki, Progress of The-

- oretical Physics Supplement **68**, 29 (1980).
 [3] F. Hoyle, Astrophys. J. Suppl. , 121 (1954).
 [4] E. Uegaki, S. Okabe, Y. Abe, and H. Tanaka, Progress of Theoretical Physics **57**, 1262 (1977).

- [5] A. Tohsaki, H. Horiuchi, P. Schuck, and G. Röpke, *Phys. Rev. Lett.* **87**, 192501 (2001).
- [6] S. Binder, J. Langhammer, A. Calci, and R. Roth, *Physics Letters B* **736**, 119 (2014).
- [7] P. Maris, J. P. Vary, and A. M. Shirokov, *Phys. Rev. C* **79**, 014308 (2009).
- [8] A. C. Dreyfuss, K. D. Launey, T. Dytrych, J. P. Draayer, and C. Bahri, *Physics Letters B* **727**, 511 (2013).
- [9] T. Yoshida, N. Shimizu, T. Abe, and T. Otsuka, *Journal of Physics: Conference Series* **569**, 012063 (2014).
- [10] T. Neff and H. Feldmeier, *Nuclear Physics A* **738**, 357 (2004), proceedings of the 8th International Conference on Clustering Aspects of Nuclear Structure and Dynamics.
- [11] M. Chernykh, H. Feldmeier, T. Neff, P. von Neumann-Cosel, and A. Richter, *Phys. Rev. Lett.* **105**, 022501 (2010).
- [12] N. Itagaki, J. Cseh, and M. Płoszajczak, *Phys. Rev. C* **83**, 014302 (2011).
- [13] N. Itagaki, H. Matsuno, and T. Suhara, *Progress of Theoretical and Experimental Physics* **2016**, 093D01 (2016).
- [14] T. Suhara, N. Itagaki, J. Cseh, and M. Płoszajczak, *Phys. Rev. C* **87**, 054334 (2013).
- [15] N. Itagaki, *Phys. Rev. C* **94**, 064324 (2016).
- [16] N. Itagaki and A. Tohsaki, *Phys. Rev. C* **97**, 014307 (2018).
- [17] N. Itagaki, H. Matsuno, and A. Tohsaki, *Phys. Rev. C* **98**, 044306 (2018).
- [18] N. Itagaki, H. Masui, M. Ito, and S. Aoyama, *Phys. Rev. C* **71**, 064307 (2005).
- [19] H. Masui and N. Itagaki, *Phys. Rev. C* **75**, 054309 (2007).
- [20] N. Itagaki, H. Matsuno, and Y. Kanada-En'yo, *Prog. Theor. Exp. Phys.* **2019** (2019), 10.1093/ptep/ptz046, 063D02.
- [21] H. Matsuno, Y. Kanada-En'yo, and N. Itagaki, *Phys. Rev. C* **98**, 054306 (2018).
- [22] N. Itagaki, H. Masui, M. Ito, S. Aoyama, and K. Ikeda, *Phys. Rev. C* **73**, 034310 (2006).
- [23] N. Itagaki and A. Tohsaki, *Phys. Rev. C* **97**, 014304 (2018).
- [24] R. Tamagaki, *Progress of Theoretical Physics* **39**, 91 (1968).
- [25] A. Volkov, *Nuclear Physics* **74**, 33 (1965).
- [26] A. Tohsaki, *Phys. Rev. C* **49**, 1814 (1994).
- [27] N. Itagaki, A. Ohnishi, and K. Kato, *Progress of Theoretical Physics* **94**, 1019 (1995).
- [28] M. Freer, H. Horiuchi, Y. Kanada-En'yo, D. Lee, and U.-G. Meißner, *Rev. Mod. Phys.* **90**, 035004 (2018).
- [29] H. Morinaga, *Phys. Rev.* **101**, 254 (1956).
- [30] M. Itoh, H. Akimune, M. Fujiwara, U. Garg, N. Hashimoto, T. Kawabata, K. Kawase, S. Kishi, T. Murakami, K. Nakanishi, Y. Nakatsugawa, B. K. Nayak, S. Okumura, H. Sakaguchi, H. Takeda, S. Terashima, M. Uchida, Y. Yasuda, M. Yosoi, and J. Zenihiro, *Phys. Rev. C* **84**, 054308 (2011).
- [31] T. Suhara and Y. Kanada-En'yo, *Phys. Rev. C* **91**, 024315 (2015).
- [32] P. Chevallier, F. Scheibling, G. Goldring, I. Plessner, and M. W. Sachs, *Phys. Rev.* **160**, 827 (1967).
- [33] A. H. Wuosmaa, R. R. Betts, B. B. Back, M. Freer, B. G. Glagola, T. Happ, D. J. Henderson, P. Wilt, and I. G. Bearden, *Phys. Rev. Lett.* **68**, 1295 (1992).
- [34] H. Flocard, P. H. Heenen, S. J. Krieger, and M. S. Weiss, *Prog. Theor. Phys.* **72**, 1000 (1984).
- [35] N. Itagaki, S. Okabe, K. Ikeda, and I. Tanihata, *Phys. Rev. C* **64**, 014301 (2001).
- [36] M. Bender and P.-H. Heenen, *Nuclear Physics A* **713**, 390 (2003).
- [37] N. Itagaki, W. von Oertzen, and S. Okabe, *Phys. Rev. C* **74**, 067304 (2006).
- [38] J. Maruhn, N. Loeb, N. Itagaki, and M. Kimura, *Nuclear Physics A* **833**, 1 (2010).
- [39] T. Suhara and Y. Kanada-En'yo, *Phys. Rev. C* **82**, 044301 (2010).
- [40] N. Furutachi and M. Kimura, *Phys. Rev. C* **83**, 021303 (2011).
- [41] T. Ichikawa, J. A. Maruhn, N. Itagaki, and S. Ohkubo, *Phys. Rev. Lett.* **107**, 112501 (2011).
- [42] J. M. Yao, N. Itagaki, and J. Meng, *Phys. Rev. C* **90**, 054307 (2014).
- [43] Y. Iwata, T. Ichikawa, N. Itagaki, J. A. Maruhn, and T. Otsuka, *Phys. Rev. C* **92**, 011303 (2015).
- [44] T. Suhara, Y. Funaki, B. Zhou, H. Horiuchi, and A. Tohsaki, *Phys. Rev. Lett.* **112**, 062501 (2014).
- [45] P. W. Zhao, N. Itagaki, and J. Meng, *Phys. Rev. Lett.* **115**, 022501 (2015).
- [46] Y. Suzuki and W. Horiuchi, *Phys. Rev. C* **95**, 044320 (2017).
- [47] T. Baba and M. Kimura, *Phys. Rev. C* **97**, 054315 (2018).
- [48] T. Inakura and S. Mizutori, *Phys. Rev. C* **98**, 044312 (2018).
- [49] Z. X. Ren, S. Q. Zhang, P. W. Zhao, N. Itagaki, J. A. Maruhn, and J. Meng, *Sci. China Phys, Mechanics & Astronomy* **62**, 112062 (2019).
- [50] R. Machleidt and D. Entem, *Physics Reports* **503**, 1 (2011).
- [51] Y. Mito and M. Kamimura, *Progress of Theoretical Physics* **56**, 583 (1976).
- [52] M. Kamimura, *Prog. Theor. Phys. Suppl.* **62**, 236 (1977).
- [53] F. Tanabe, A. Tohsaki, and R. Tamagaki, *Progress of Theoretical Physics* **53**, 677 (1975).
- [54] N. P. Heydenburg and G. M. Temmer, *Phys. Rev.* **104**, 123 (1956).
- [55] J. L. Russell, G. C. Phillips, and C. W. Reich, *Phys. Rev.* **104**, 135 (1956).
- [56] R. Nilson, W. K. Jentschke, G. R. Briggs, R. O. Kerman, and J. N. Snyder, *Phys. Rev.* **109**, 850 (1958).
- [57] C. M. Jones, G. C. Phillips, and P. D. Miller, *Phys. Rev.* **117**, 525 (1960).
- [58] K. Miyake, *Bulletin of the Institute for Chemical Research, Kyoto University* **39**, 313 (1961).
- [59] T. A. Tombrello and L. S. Senhouse, *Phys. Rev.* **129**, 2252 (1963).
- [60] A. D. Bacher, F. G. Resmini, H. E. Conzett, R. de Swiniarski, H. Meiner, and J. Ernst, *Phys. Rev. Lett.* **29**, 1331 (1972).
- [61] M. Freer, J. D. Malcolm, N. L. Achouri, N. I. Ashwood, D. W. Bardayan, S. M. Brown, W. N. Catford, K. A. Chipps, J. Cizewski, N. Curtis, K. L. Jones, T. Munoz-Britton, S. D. Pain, N. Soić, C. Wheldon, G. L. Wilson, and V. A. Ziman, *Phys. Rev. C* **90**, 054324 (2014).